





Report no.

**IPR-08-08**

Author

**Margareta Lönnqvist**

**Ola Kristensson**

**Harald Hökmark**

Checked by

**Rune Glamheden**

Approved

**Anders Sjöland**

No.

**SU448**

Date

**April 2008**

Date

**Maj 2008**

Date

**2008-06-03**

# Äspö Hard Rock Laboratory

## CAPS – Confining Application to Prevent Spalling

### Scoping calculations – Field test at Äspö HRL

Margareta Lönnqvist

Ola Kristensson

Harald Hökmark

Clay Technology AB

April 2008

**Keywords:** Thermo-mechanical stress, Spalling, Deposition hole configuration, Tunnel floor geometry, Scoping calculations, CAPS, Code\_Bright

This report concerns a study which was conducted for SKB. The conclusions and viewpoints presented in the report are those of the author(s) and do not necessarily coincide with those of the client.



# Abstract

The CAPS (Confining Application to Prevent Spalling) field test aims to investigate whether small pressures acting on the deposition hole wall can prevent or minimize the spalling initiation process.

This report includes numerical simulations of the thermo-mechanical evolution of the stresses in the CAPS field test. A linear elastic, 3D Code\_Bright finite element continuum model was used in the numerical calculations.

The main issue was to determine the optimal hole configuration, from a number of suggestions, such that the risk and extent of spalling during drilling was minimized and the highest possible stresses were achieved during the subsequent heating phase. The effects of having rounded or flat floors in the tunnel were compared.

Hole configurations with pairs of holes on either side of the tunnel axis were found to be optimal. The exact geometry of the tunnel floor was found to be of minor importance.



# Sammanfattning

Fältförsöket CAPS (Confining Application to Prevent Spalling) i Äspö HRL syftar till att undersöka om små mothåll i deponeringshålen kan förhindra eller undertrycka uppkomsten av termiskt inducerad spjälkning.

Denna rapport behandlar numerisk simulering av den termomekaniska utvecklingen hos spänningarna i fältförsöket CAPS. Till de numeriska beräkningarna användes en linjärelastisk, 3-dimensionell Code\_Bright finita-element-kontinuummodell.

Huvuduppgiften var att undersöka vilken av de föreslagna hålkonfigurationerna som minimerade risken för spjälkning under borrningen och gav de största spänningarna under uppvärmningsfasen. Även inflytandet av rundat respektive plant tunnelgolv studerades.

Resultaten visar att hålkonfigurationen med ett deponeringshål på var sin sida av tunnelaxeln är optimal. Den exakta golvgeometrin visade sig ha mycket liten effekt på spänningarna.



# Contents

<b>1</b>	<b>Introduction</b>	<b>9</b>
<b>2</b>	<b>Geometry</b>	<b>11</b>
<b>3</b>	<b>Rock properties, in situ stress state and thermal load</b>	<b>15</b>
3.1	Simulation setup	16
<b>4</b>	<b>Results</b>	<b>17</b>
4.1	Base case	17
4.2	Sensitivity analyses	22
4.2.1	Pillar width analysis	22
4.2.2	Variation in thermal conductivity	23
4.2.3	Variations in Young's modulus	25
4.2.4	Variation in tunnel geometry	26
<b>5</b>	<b>Conclusions</b>	<b>29</b>
	<b>References</b>	<b>31</b>
<b>A</b>	<b>Influence of the shape of the tunnel cross section on the major principal stress</b>	<b>35</b>
A.1	Idealized tunnel shape	36
A.2	Real tunnel shape	37



# 1 Introduction

The CAPS field experiment is being planned to take place in the Q-tunnel, at the Äspö HRL. A number of 0.5 m diameter, 4 m deep holes will be excavated and subsequently heated with central heaters. There may be individual holes and pairs of holes separated by a pillar. The experiment objective is to establish whether or not a small support pressure will suppress or inhibit spalling. This document compiles results from a first set of scoping calculations, aimed at getting a first perception of how the hole location, the pillar width and the heat load should be specified to give tangential stress conditions as similar as possible to those of KBS-3 deposition holes.

All analyses were performed with Code\_Bright /CIMNE, 2004/.

A set of possible hole configurations has been suggested by Glamheden /2007/, see Figure 1-1.

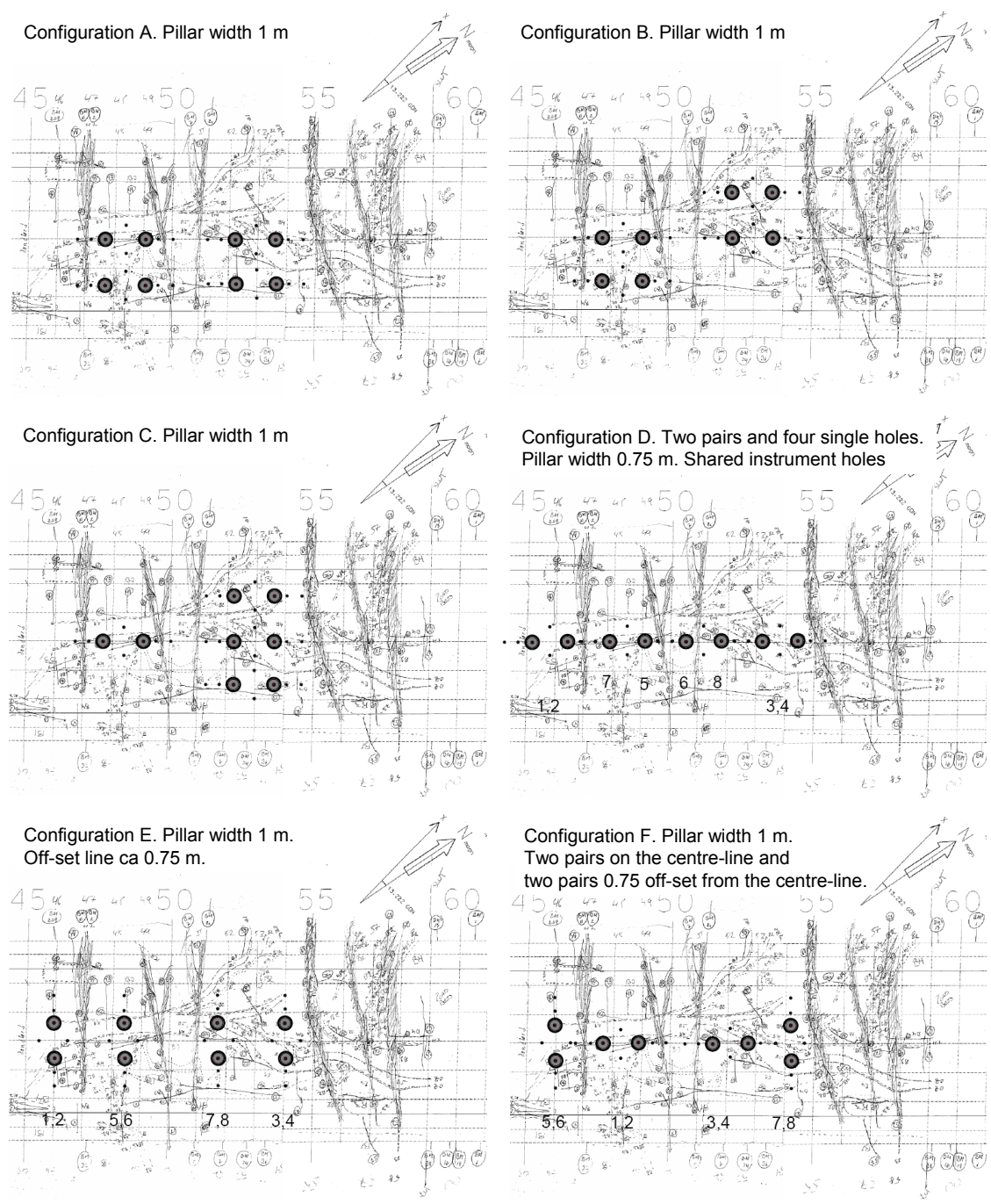


**Figure 1-1.** Suggested hole configurations.

## 2 Geometry

Four different hole configurations have been investigated:

- Model D1: One single centred hole (Configuration D, see Figure 2-1)
- Model F1: A pair of centred holes with 1 m pillar (Configuration F, see Figure 2-2).
- Model F2: A pair of centred holes with 0.6 m pillar (see Figure 2-3).
- Model F3: A pair of holes, one on each side of the tunnel axis, with 1 m pillar (Configuration F, Figure 2-4).

The various hole configurations shown in Figure 1-1 are summarized in Table 2-1, together with the models analysed so far. Note that Configuration D, with a pair of centred holes, has a pillar width that is between the corresponding widths in Models F1 and F2. The different geometries are presented in Figure 2-1, Figure 2-2, Figure 2-3, Figure 2-4, and Figure 2-5 below. Models F1 and F2 do not take full advantage of the symmetry of the hole configurations. Their geometries were created with the intention that, with some modification, hole configurations without full symmetry could be investigated.

**Table 2-1. Hole configuration and preliminary model map.**

<b>Model Code</b>	<b>Pillar width</b>	<b>Position</b>	<b>Hole configuration</b>
D1	-	Single hole on tunnel axis	D
F1	1 m	Pair of holes on tunnel axis	A, B, C, E, F
F3	1 m	Pair of holes on either side of tunnel axis	E, F
F2	0.6 m	Pair of holes on tunnel axis	-

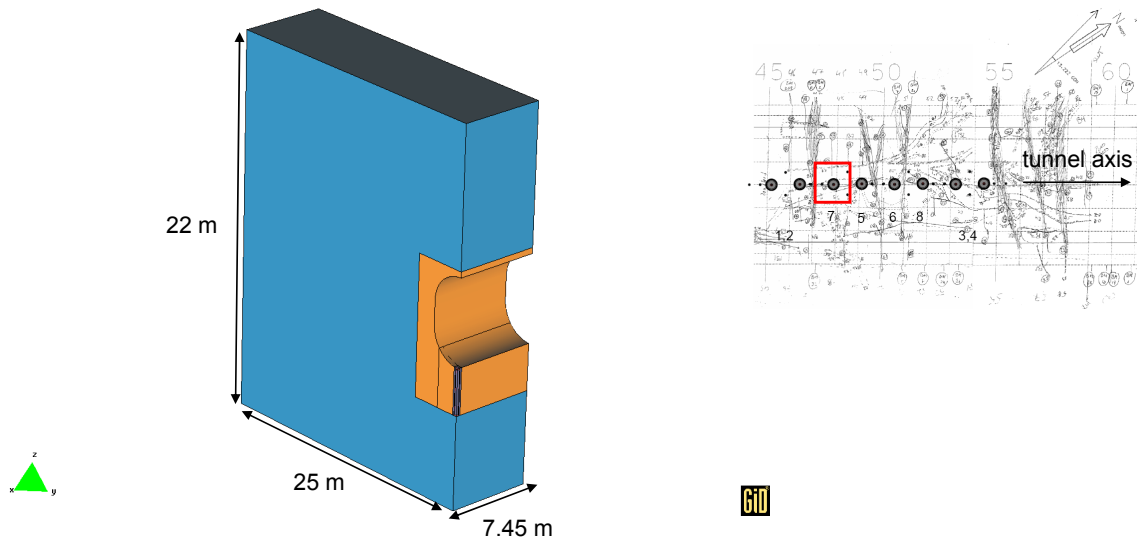


**Figure 2-1.** Model D1: Geometry and dimension for the case with one single hole on the tunnel axis. Holes other than the specifically marked ones are ignored.

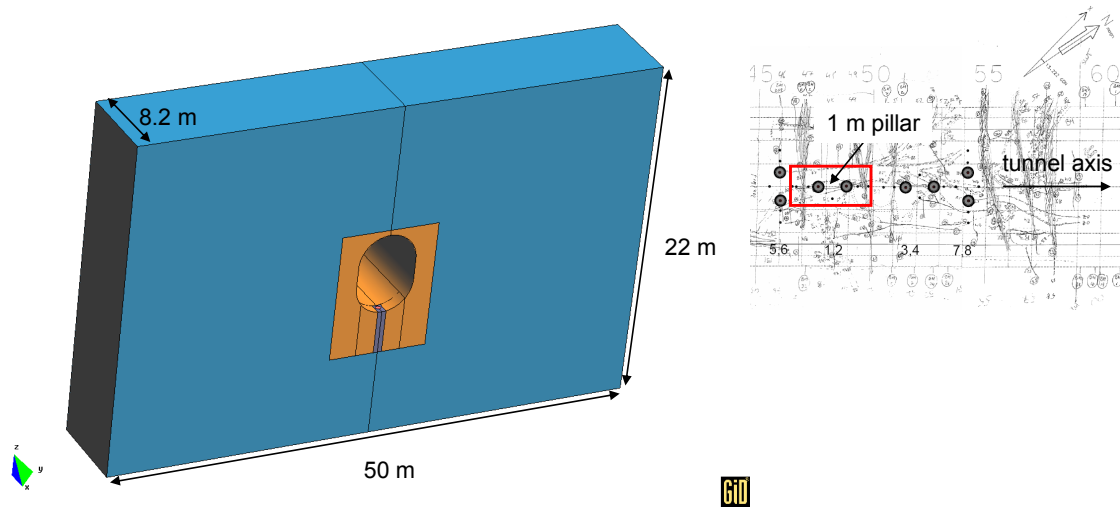


**Figure 2-2.** Model F1: Geometry and dimension for the case with centred holes with 1 m pillar. Holes other than the specifically marked ones are ignored.

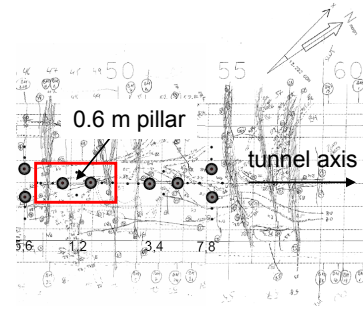
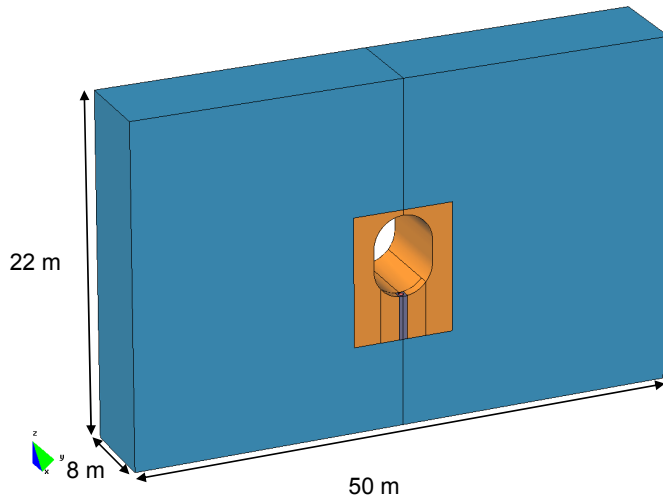


**Figure 2-3.** Model F2: Geometry and dimension for the case with centred holes with 0.6 m pillar. Holes other than the specifically marked ones are ignored.

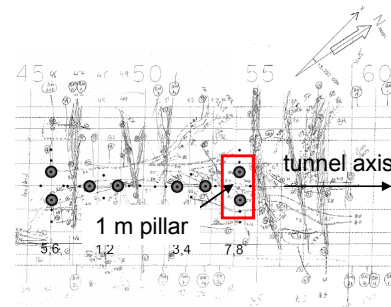
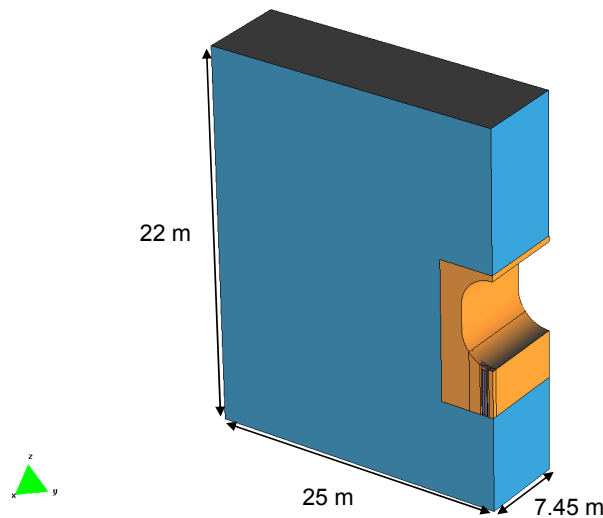


**Figure 2-4.** Model F3: Geometry and dimension for the case with a pair of holes, one on each side of the tunnel axis, with 1 m pillar. Holes other than the specifically marked ones are ignored.

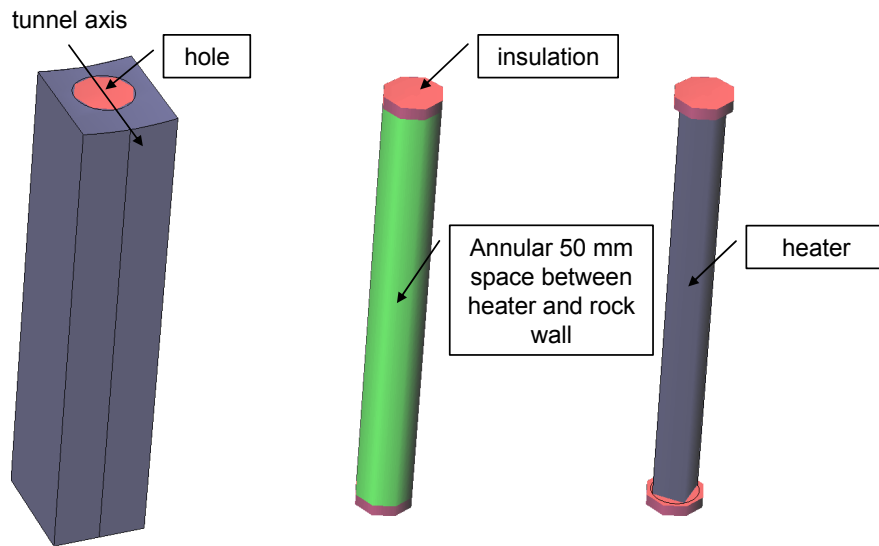


**Figure 2-5.** Hole configuration. Left: Volume of rock surrounding the hole. Middle: Annular space between heater and rock with insulation on top and bottom. Right: Heater with (the same) insulation on top and bottom.

### 3 Rock properties, in situ stress state and thermal load

In Andersson /2007/ the geology of the APSE tunnel is quite extensively described as well as the in situ stress state and the means used to determine it. The rock properties and the stress state around the tunnel are summarized in the tables below.

**Table 3-1. Material properties. Values in brackets are fictitious material properties used during the excavation phase to minimize the influence on the stresses around the deposition hole.**

Material property	Rock	Annular space between rock and heater 1)	Insulation	Heater
$\rho$ [kg/m <sup>3</sup> ]	2730	2780	20	7500
$C$ [J/(kg·K)]	770	800	5000	500
$\lambda$ [W/(m·K)]	3.2	0.3	0.04	40
$E$ [GPa]	55	(0.076) 0.1	0.02	(0.076) 200
$\nu$ [-]	0.25	0.25	0.25	0.25
$\alpha$ [1/K]	7.00E-06	7.00E-06	3.00E-04	1.00E-05
$n$ [-]	0	0.6	0	0

1) Here, the material properties are those of bentonite pellets. In the tangential stress results presented in the following we have added the radial stress generated in the interior of the hole to capture the conditions in un-filled holes. The compensation is however, very minor (2.5 MPa). The mechanical parameter values given for the heater-rock space are not important to the results presented in the following.

The tunnel is orientated such that the major principal stress is perpendicular to the tunnel axis. Here, the intermediate principal stress corresponds to the vertical stress.

**Table 3-2. Back-calculated and best-estimate stress state for the APSE site, /Andersson, 2007/.**

	$\sigma_1$	$\sigma_2$	$\sigma_3$
Magnitude [MPa]	30	15	10
Trend (Äspö 96)	310	090	220

In APSE a tangential stress of approximately 120 MPa appeared to initiate the spalling process in the unsupported hole. The tangential stresses found here are compared with that spalling threshold.

The CAPS heaters are modelled as cylinders of 3.8 m height, positioned 0.1 m above the deposition hole floor. In all models, the heater has a power of 500 W/m.

The initial undisturbed temperature is set at 15°C in all models.

### **3.1 Simulation setup**

The simulations are performed in the two main steps below:

1. The stress field after excavation is obtained performing the following steps.
  - a. Apply the homogenous in-situ stress field on the excavated geometry. Impose zero traction on the tunnel surface created by the excavations. Assign the materials in the deposition hole (annular space, insulation and heater) with low stiffness as compared to the surrounding rock mass.
  - b. Calculate the equilibrium stresses.
2. The simulation of the thermally induced stress field is started after the initial excavation-step.
  - a. The materials in the deposition hole are assigned representative stiffness.
  - b. The model is analyzed according to the heat load schedule.

## 4 Results

### 4.1 Base case

The results from Models D1, F1, F2 and F3 are presented below. The temperature distribution around one deposition hole in a horizontal cross section 2 m below the tunnel floor is shown in Figure 4-1, Figure 4-2, Figure 4-3 and Figure 4-4.

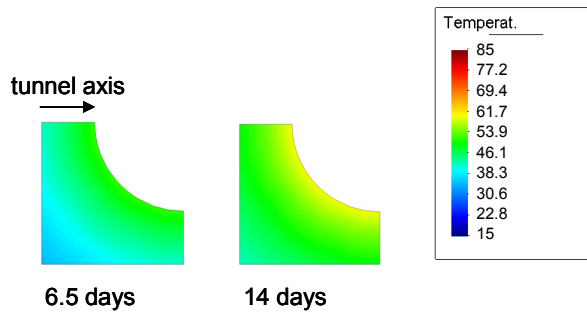


**Figure 4-1.** Model D1: Temperature distribution around one deposition hole 2 m below the tunnel floor after 6.5 days and 14 days of heating.

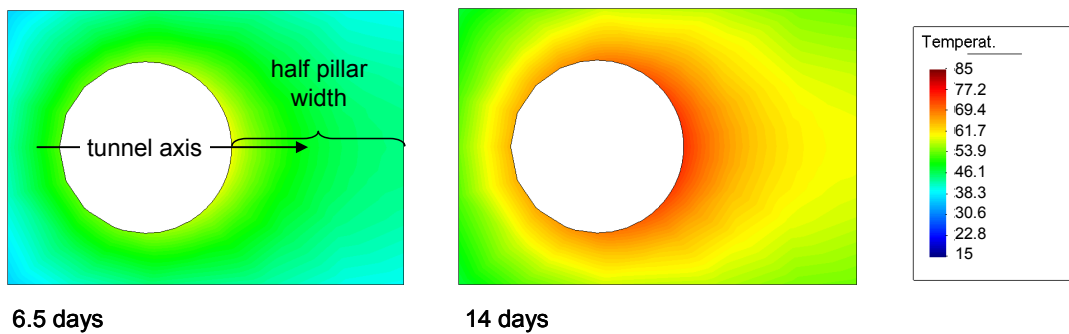


**Figure 4-2.** Model F1: Temperature distribution around one deposition hole 2 m below the tunnel floor after 6.5 days and 14 days of heating.

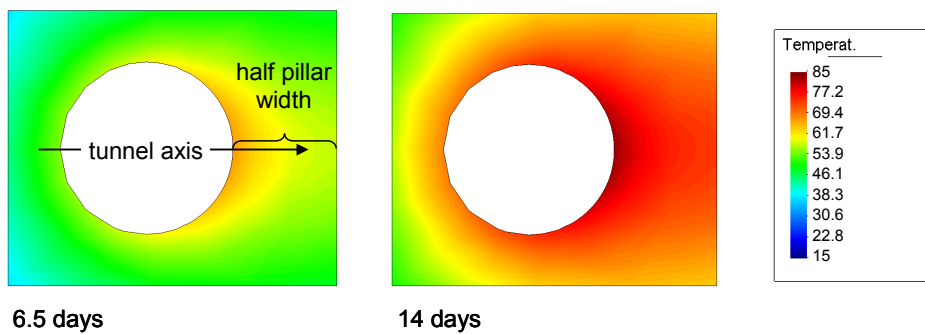


**Figure 4-3.** Model F2: Temperature distribution around one deposition hole 2 m below the tunnel floor after 6.5 days and 14 days of heating.

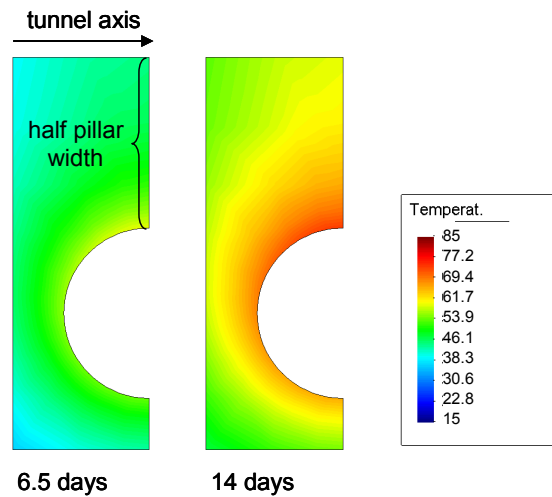


**Figure 4-4.** Model F3: Temperature distribution around one deposition hole 2 m below the tunnel floor after 6.5 days and 14 days of heating.

In all four deposition hole configurations the major principal stress is found at positions, on the hole perimeter, parallel to the tunnel axis, cf. Figure 4-5. There does not seem to be any rotation of the position of the major principal stress as the hole is moved off the tunnel axis.

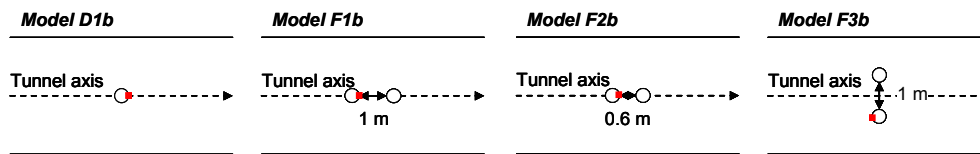


**Figure 4-5.** Model hole configurations with location (red symbol) of major principal stress after excavation and subsequent heating.

The major principal stress along a vertical scan-line on the deposition hole perimeter is shown in the figures below. Figure 4-6 shows the temporal development of the stresses in each of the hole configurations. Figure 4-7 shows a comparison between the models.

Of the four models studied here, Model F3 (with a pair of holes on either side of the tunnel axis) has the smallest stresses after excavation. The models with either a single centred hole (Model D1) or a centred pair with 1 m pillar (Model F1) have almost equal stresses. A longer heating period than 14 days would induce higher stresses in the model with a pair of holes than in the one with a single hole. The spalling strength (120 MPa) is exceeded in all three models to depths of at least 2.5 m below the tunnel floor after 14 days of heating.

The stresses in the centre of the pillar in Models F1, F2 and F3 are presented in Figure 4-8. Here,  $\sigma_h$  is the horizontal stress along the tunnel,  $\sigma_H$  is the horizontal stress across tunnels and  $\sigma_z$  is the vertical stress. Model F3 (a pair of holes on either side of the tunnel axis) has considerably smaller stresses than the other two models in the centre of the pillar.

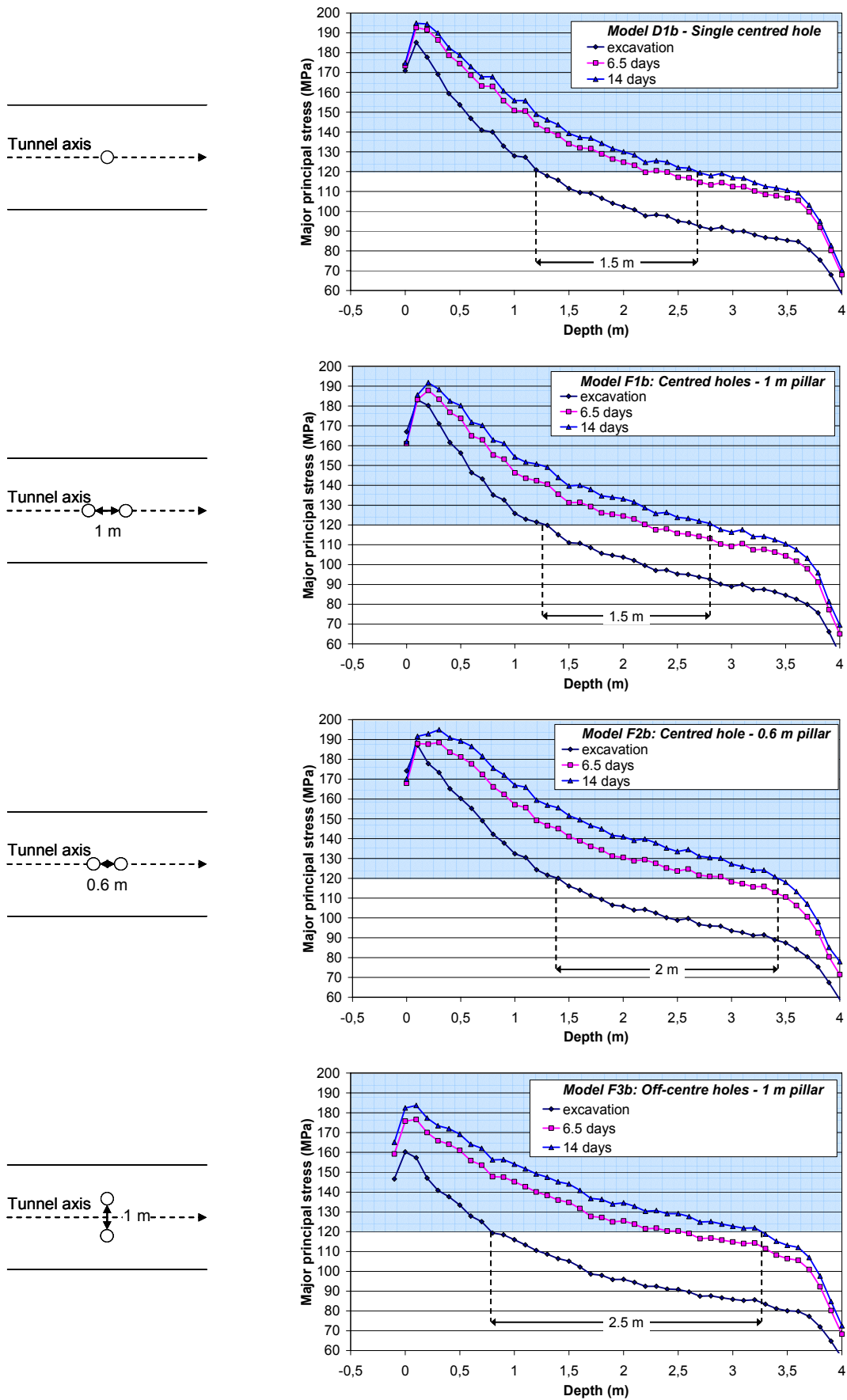


**Figure 4-6.** Temporal development of the major principal stress along the deposition hole wall. Stresses exceeding the assumed spalling strength are marked in blue.

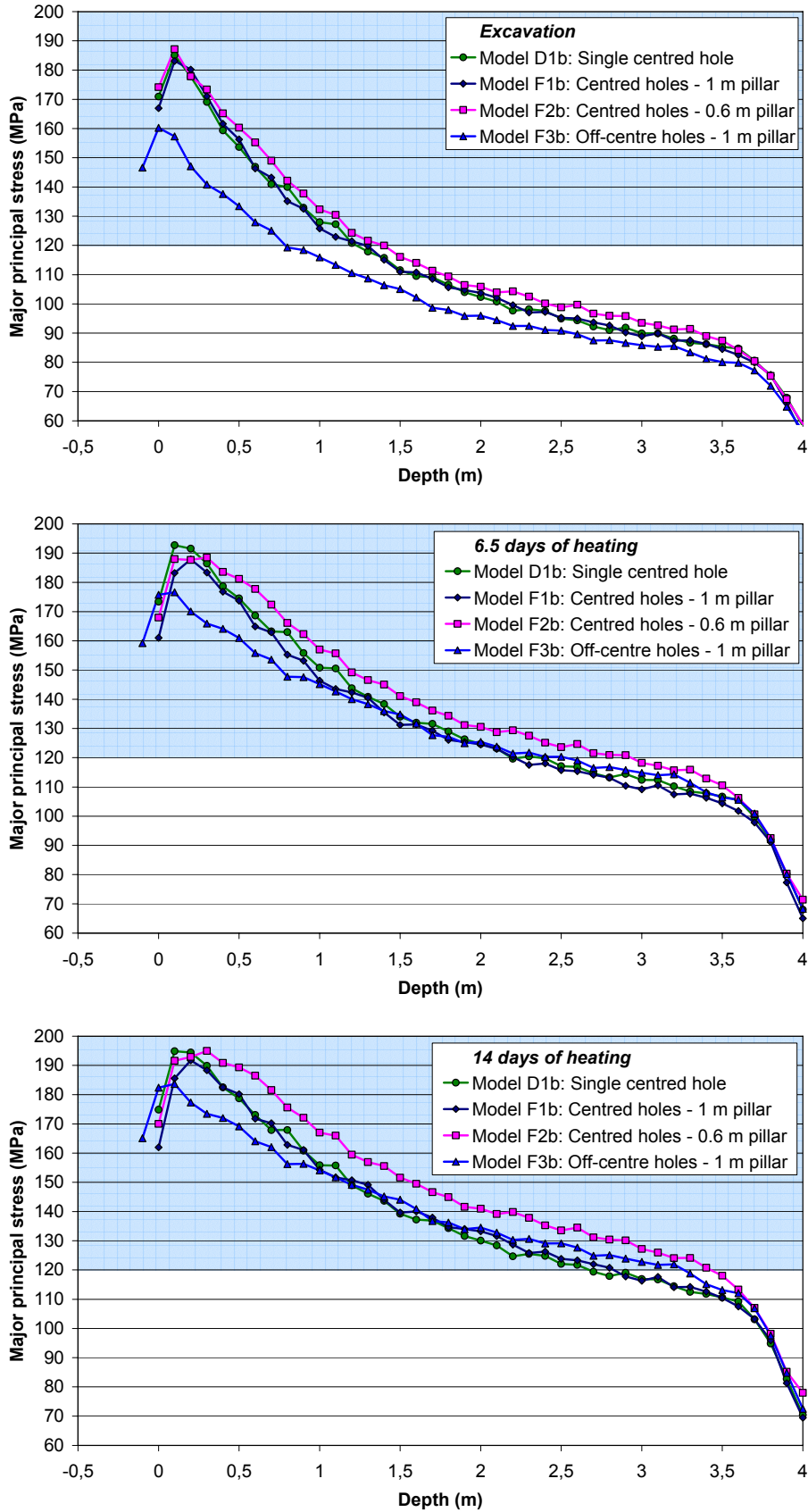


**Figure 4-7.** Comparison between major principal stress in each of the three models after excavation (top), 6.5 days of heating (middle) and 14 days of heating (bottom). Stresses exceeding the assumed spalling strength are marked in blue.

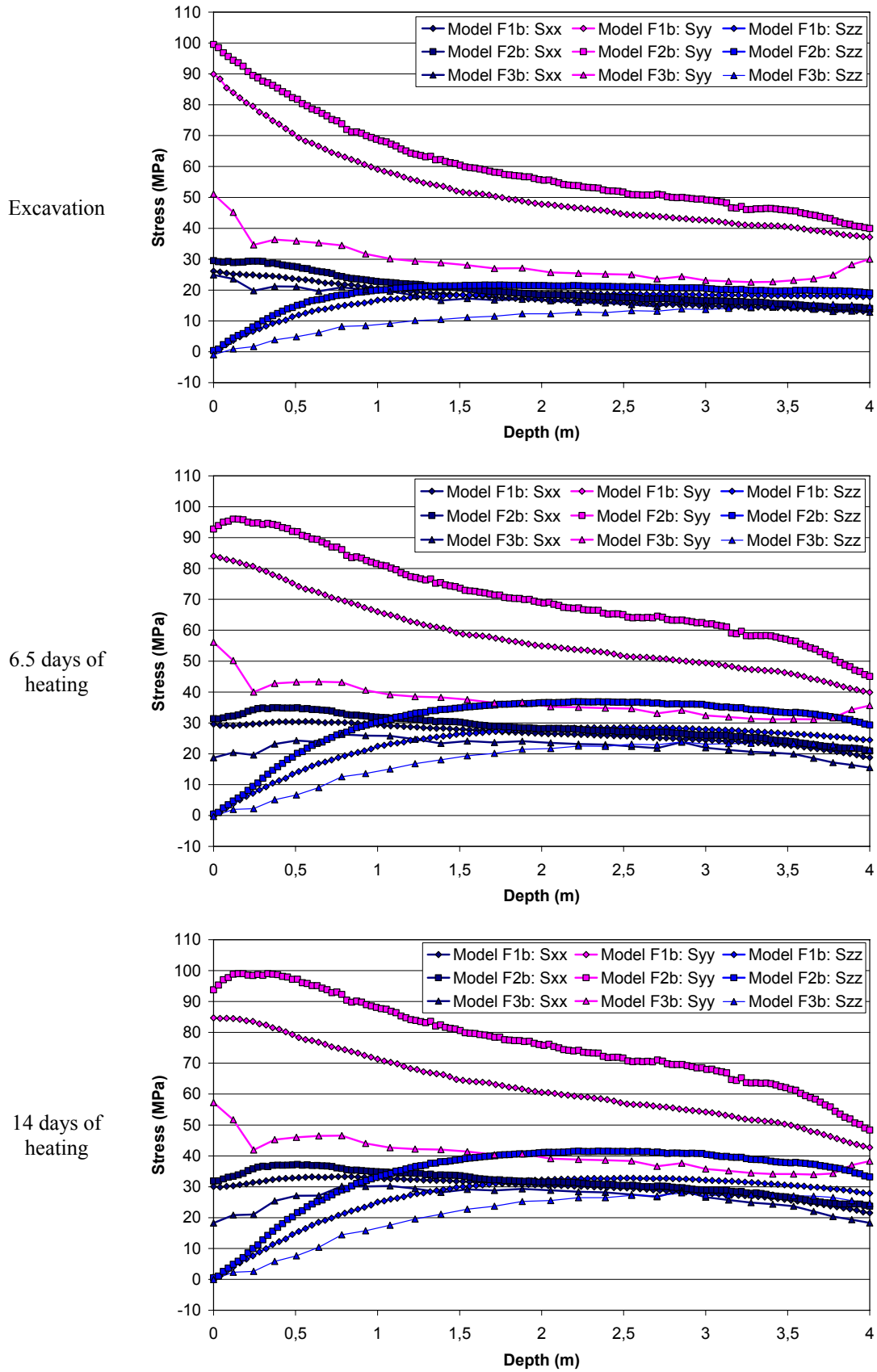


**Figure 4-8.** Comparison between the stresses at the centre of the pillar in each of the models after excavation (top), 6.5 days of heating (middle) and 14 days of heating (bottom).

## 4.2 Sensitivity analyses

### 4.2.1 Pillar width analysis

The drill plan for the CAPS pilot holes included 4 pairs of holes with each pair oriented normal to the tunnel axis and with a 1.0 m pillar between the holes (see Figure 4-8). Results from the previous section have shown that this configuration would minimize the tangential stresses after excavation (see Figure 4-7, top) and at the same time give large enough stresses after a period of heating to allow for relevant spalling observations. In the current section, the effects of reducing the pillar width in hole configuration E will be investigated.

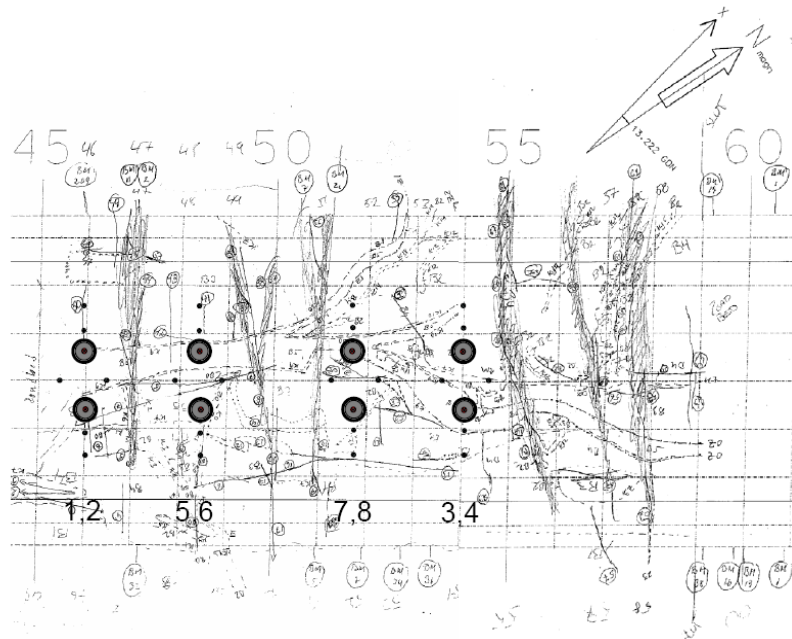


**Figure 4-9.** Suggested hole configuration E.

Figure 4-10 shows the development of the major principal stress along the deposition hole wall for the cases with a pair of holes on each side of the tunnel with either a 1 m pillar width (Model F3b) or 0.7 m (Model F4b).

As seen in the figure, there is a moderate (about 5 MPa) increase in the stresses in the upper part of the hole. However, this increase is only seen where the stresses have already exceeded the assumed spalling strength. Consequently, reducing the pillar width from 1 m to 0.7 m will not have a negative impact on the experiment.

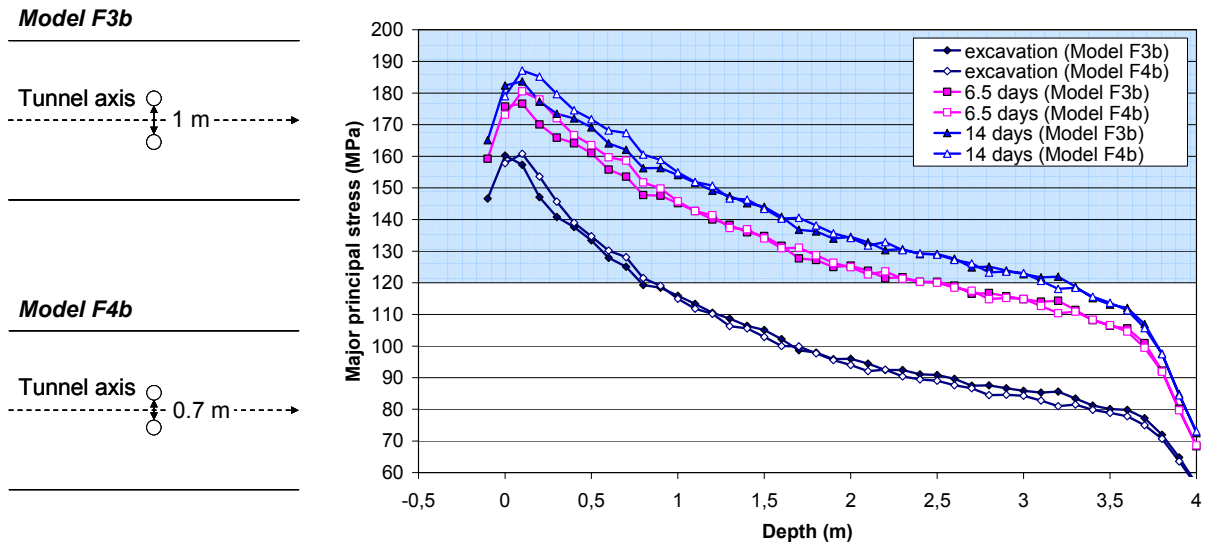


**Figure 4-10.** Temporal development of the major principal stress along the deposition hole wall. Stresses exceeding the assumed spalling strength are marked in blue.

#### 4.2.2 Variation in thermal conductivity

The thermal conductivity of Äspö diorite has a mean value of 2.7 W/(m·K) (it ranges between 2.39-2.80 W/(m·K)) /Andersson, 2007/. However, in the thermal modelling of the APSE experiment, the value 3.2 W/(m·K) was used as it was found to give a better fit to the measured temperatures /Fälth *et al.*, 2005/. A comparison between the two thermal conductivities is shown in Figure 4-11. As seen in the figure, the reduced value of the thermal conductivity results in an increase in the major principal stress by about 5 MPa.

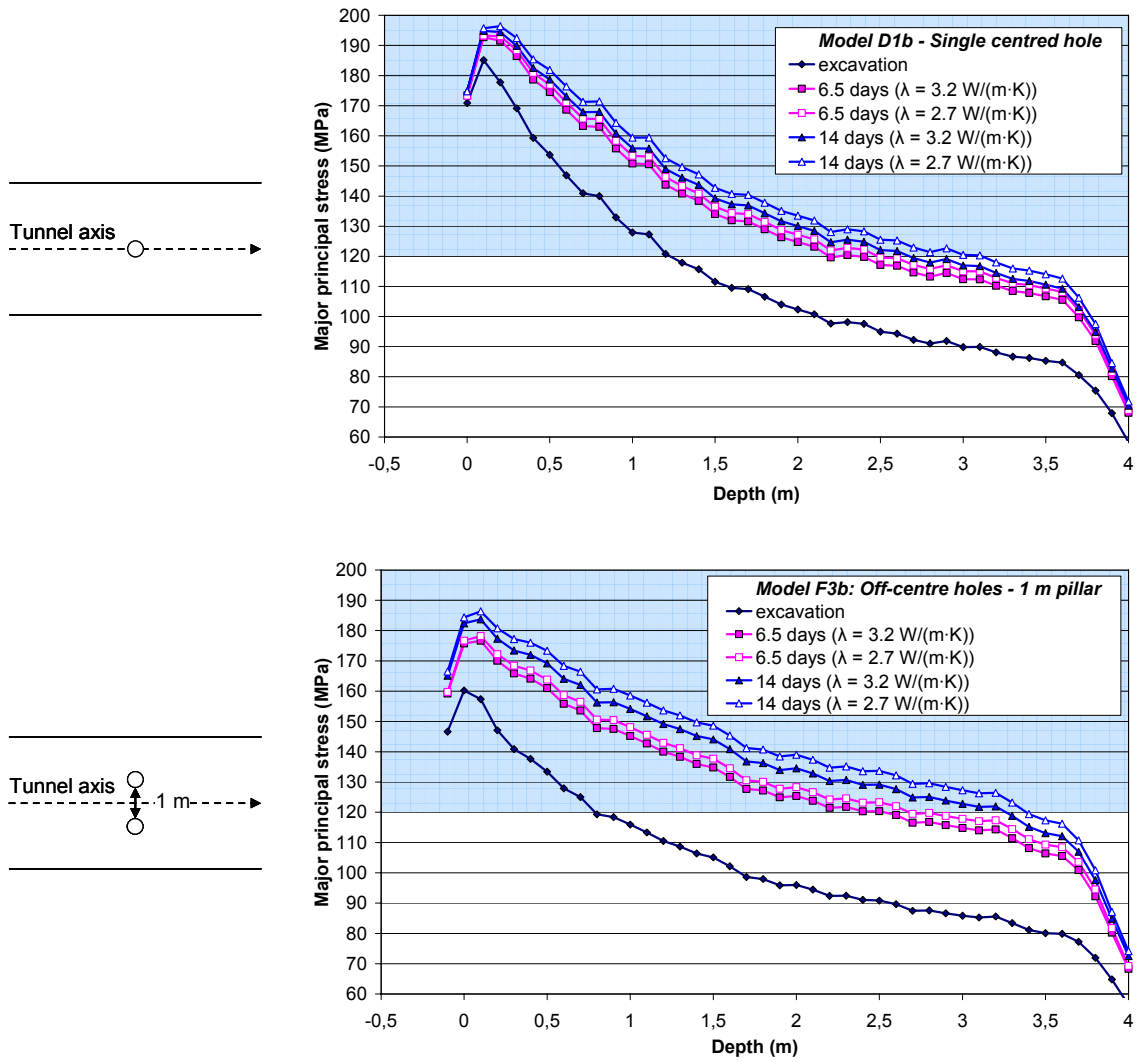


**Figure 4-11.** Temporal development of the major principal stress along the deposition hole wall. Stresses exceeding in the assumed spalling strength are marked in blue.

### 4.2.3 Variations in Young's modulus

The values of Young's modulus, at Äspö HRL, are 76 GPa (for intact rock) and 55 GPa (for rock mass) /Andersson, 2007/. A comparison between the stresses in rock with Young's modulus 55 GPa and 65.5 GPa (mean value of intact rock and rock mass) is shown in Figure 4-12.

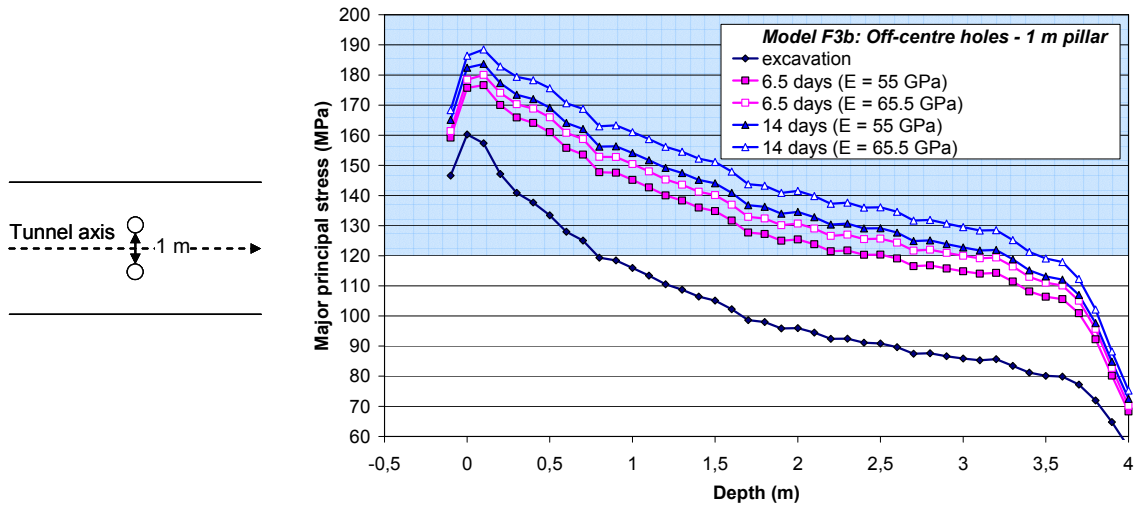


**Figure 4-12.** Temporal development of the major principal stress along the deposition hole wall. Stresses exceeding the assumed spalling strength are marked in blue.

#### 4.2.4 Variation in tunnel geometry

Figure 4-13 shows a laser-scanned profile of the floor in the Q-tunnel at Äspö HRL. As indicated in the PM presented in the Appendix to this report, a flatter tunnel floor does not seem to affect the major principal stress in any significant way at positions deeper than 1.5 m below the tunnel floor. This is confirmed in Figure 4-14, where the thermally induced stresses along the deposition hole wall, for the two floor geometries denoted A and B, are compared. Geometry A is the oval shaped tunnel cross section used in all previous models (corresponds to tunnel segments 50-55 in the Q-tunnel). Geometry B has a flat floor (corresponds to tunnel segments 46-49 in the Q-tunnel).

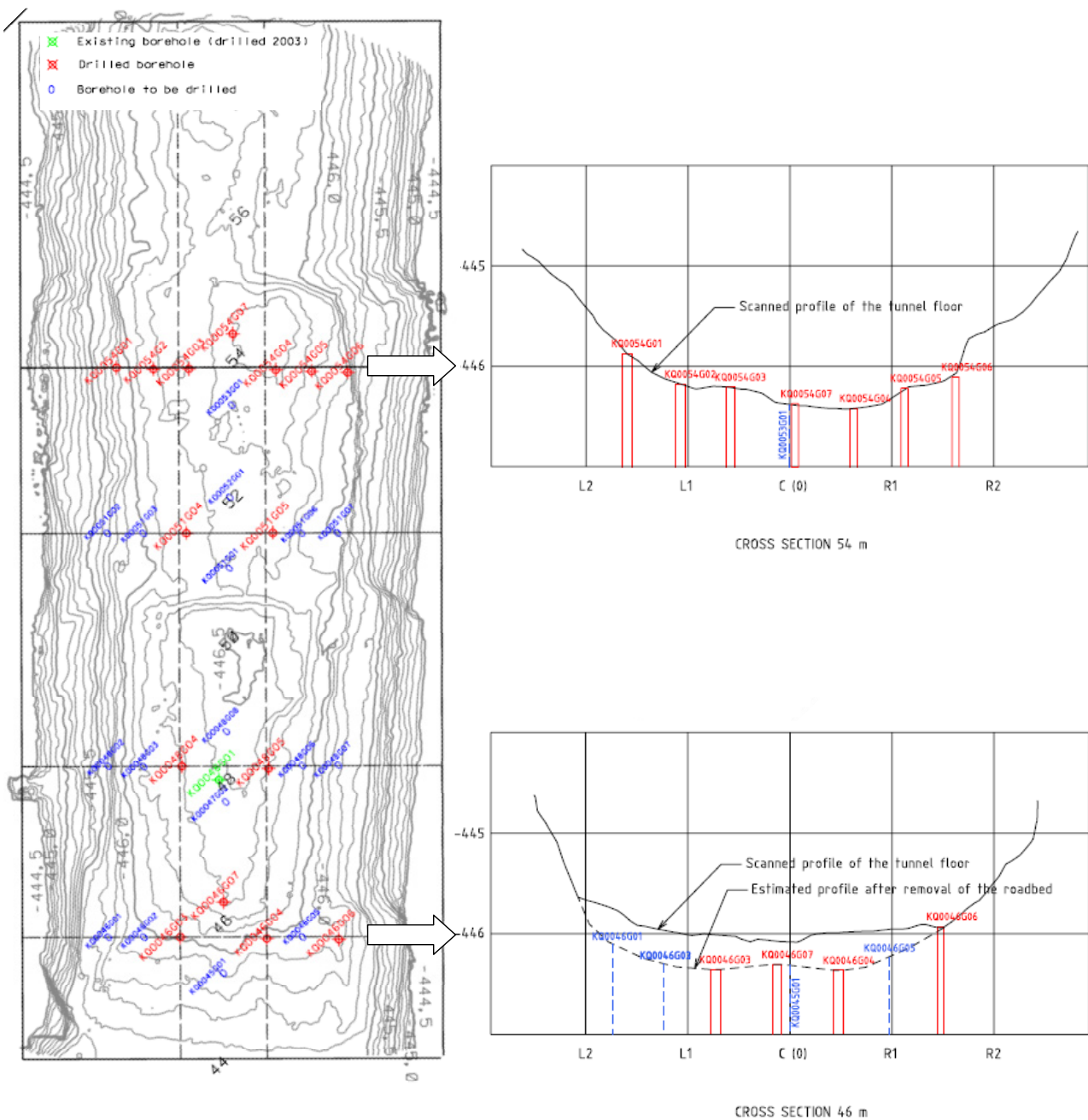
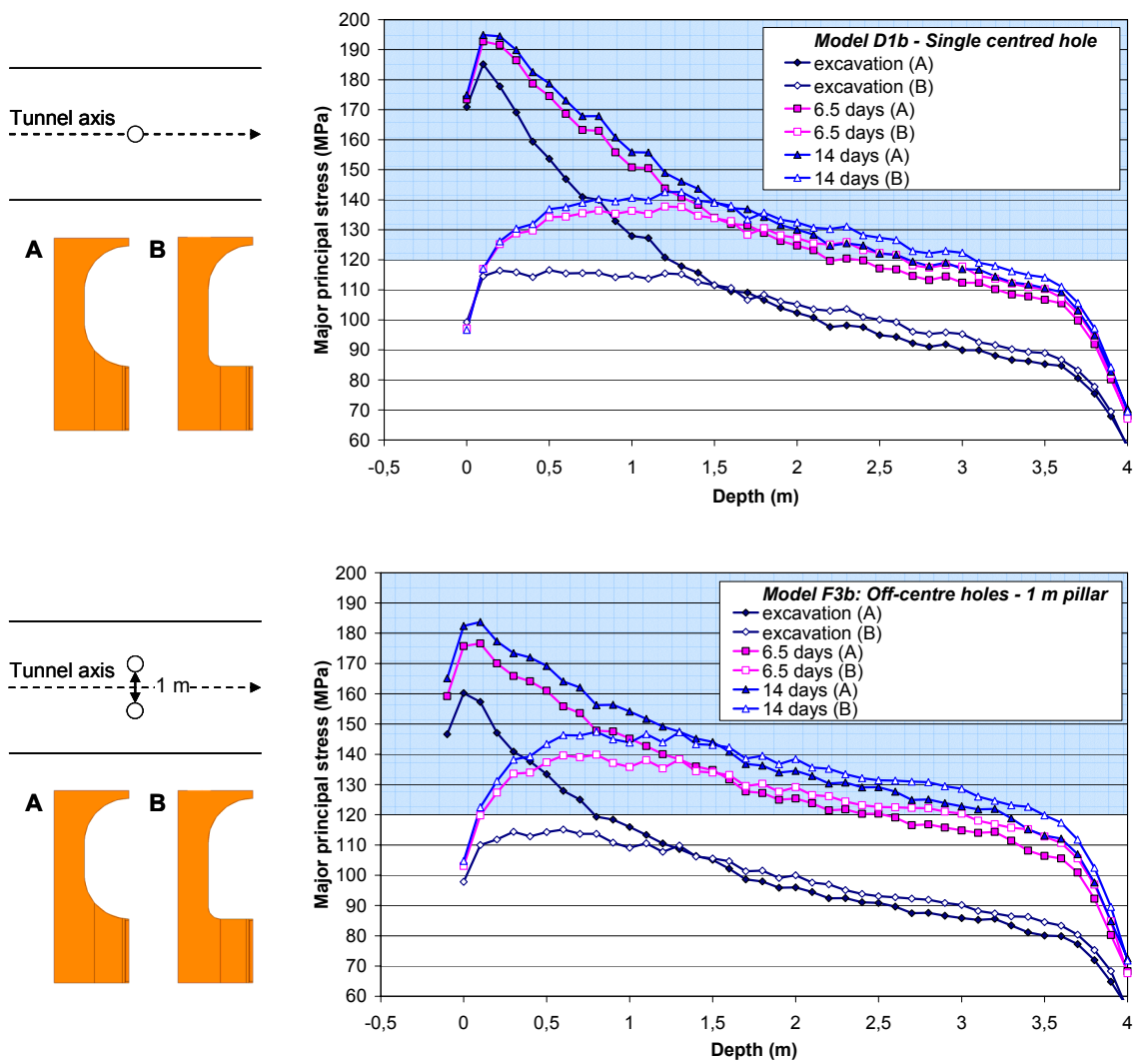


Figure 4-13. Laser-scanned floor profile in the Q-tunnel. From /Glamheden, 2008/.



**Figure 4-14.** Temporal development of the major principal stress along the deposition hole wall. Stresses exceeding the assumed spalling strength are marked in blue.



## 5 Conclusions

Out of the geometries tried here (one single hole on tunnel axis, pair of holes on axis, pair of holes aligned perpendicular to tunnel axis), the one with the pair of holes aligned perpendicular to the tunnel axis gives the largest height section available for thermally induced spalling (cf. Figure 4-6), provided that the spalling strength is about 120 MPa (cf. /Andersson, 2007/). In the uppermost part of the hole, the spalling strength is likely to be exceeded already after drilling. However, the Excavation Disturbed Zone (EDZ) in the tunnel floor might reduce the stresses in this part of the holes such that spalling does not occur. This was the case for the APSE experiment, where the top 0.5 m appeared to be free of spalling /Andersson, 2007/.

Decreasing the pillar width from 1.0 m to 0.7 m in the configuration with holes aligned perpendicular to the tunnel axis will result in moderate increase of the stresses in the upper parts of the hole.

The above also seems to be true in regions of the tunnel with a flat floor (cf. Section 4.2.4; Appendix A). Here, the stresses in the upper 1.5 m of the hole are reduced compared with those in the oval-shape reference tunnel and it is possible that spalling might be avoided after excavation, regardless of the EDZ. In the lower parts of the hole the stresses are almost equal.

Reasonable variations in Young's modulus and the thermal conductivity are unlikely to have any significant implications on the stresses. A variation in thermal conductivity in the range 2.7-3.2 W/(m·K) results in variations of the major principal stress of around 5 MPa. The corresponding variation, if the value of Young's modulus is in the range 55-65 GPa, is around 7 MPa.



## References

**Andersson J C, 2007.** Äspö Hard Rock Laboratory, Äspö Pillar Stability Experiment, Final report, Rock Mass Response to Coupled Mechanical Thermal Loading, SKB TR-07-01, Svensk Kärnbränslehantering AB.

**CIMNE, 2004.** Code\_Bright. Version 2.2 users guide. Departamento de Ingenieria del Terreno, Cartográfica y Geofísica. Universidad de Cataluña.

**Fälth B, Kristensson O, Hökmark H, 2005.** Äspö Hard Rock Laboratory. Äspö Pillar Stability Experiment. Thermo-mechanical 3D back analyze of the heating phase. SKB IPR-05-19, Svensk Kärnbränslehantering AB.

**Glamheden R, 2008.** Golder Associates AB, Uppsala. E-mail communication.

**Mas Ivars D, 2008.** ITASCA Geomekanik AB, Solna. E-mail communication.



# Appendix

## **On the influence of the tunnel shape on the major principal stress in the floor of the Q-tunnel**

Margareta Lönnqvist, Clay Technology AB

February 7, 2008



## A Influence of the shape of the tunnel cross section on the major principal stress

The actual tunnel cross section has been obtained from laser scanning sections of the Q-tunnel at Äspö HRL. Figure A-1 shows a comparison between an idealized tunnel shape and the actual tunnel shape as represented in 3DEC /Mas Ivars, 2008/. In tunnel segments 46-49 the floor appears to be rather flat compared with the other sections, which tend to be more like the idealized tunnel floor.

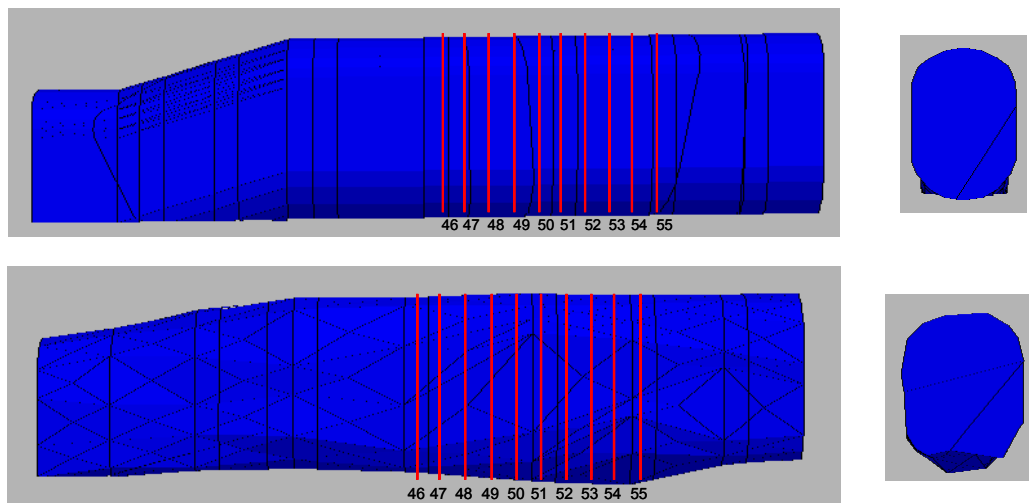


**Figure A-1.** 3DEC figures by /Mas Ivars, 2008/ – tunnel segments indicated in red. Top: Idealized tunnel shape. Bottom: Laser scanned tunnel shape.

In the following sections, the major principal stress on vertical scan-lines (also provided by /Mas Ivars, 2008/), starting at the floor of the tunnel and extending about 6 m downwards, are compared between the two 3DEC models (and with corresponding Code\_Bright results). In every tunnel segment three scan-lines are chosen: One on the tunnel axis (denoted ‘middle’) and two at positions 1.25 m on either side of the tunnel axis (denoted ‘left’ and ‘right’, respectively). Here, zero depth represents the tunnel floor in the centre of the tunnel in each segment.

The results show that there is a very minor influence on the major principal stress, at positions 1 m below the tunnel floor, of the variation in the floor geometry. It seems that there is no strong need now to perform scoping analyses of specific CAPS hole Code\_Bright models with a flat floor.

## A.1 Idealized tunnel shape

Figure A-2 shows the idealized tunnel cross sections as represented in Code\_Bright and 3DEC. Figure A-3 shows a comparison between the stresses obtained in the idealized models. As seen in the figure, there is an almost perfect agreement between the results.

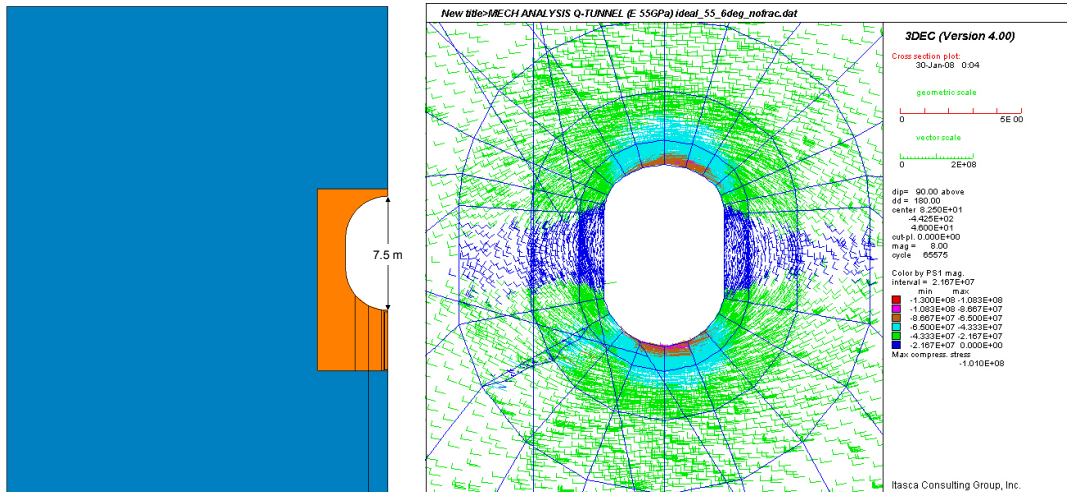


*Figure A-2. Idealized tunnel shape: Representation in Code\_bright (left). Representation in 3DEC (right).*

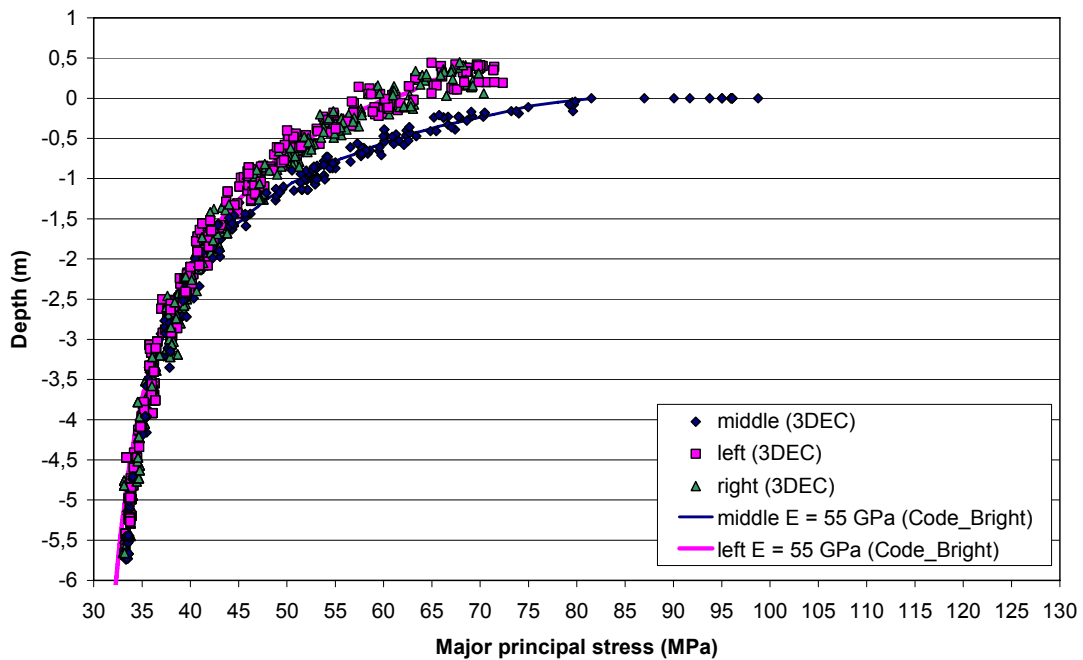


*Figure A-3. Comparison between stress magnitudes in Code\_Bright and 3DEC. 3DEC results from /Mas Ivars, 2008/.*

## A.2 Real tunnel shape

The major principal stress, along vertical scan-lines, in tunnel sections 46 to 55 is presented in Figure A-4. The stress magnitudes in the laser scanned tunnel cross sections (3DEC models by Diego Mas Ivars) are compared with results from the idealized tunnel (Code\_Bright).

As seen in the figures, at positions 1 m below the tunnel floor, the stresses in the idealized Code\_Bright model are in good agreement with the corresponding stresses in the 3DEC model with the laser scanned cross sections.

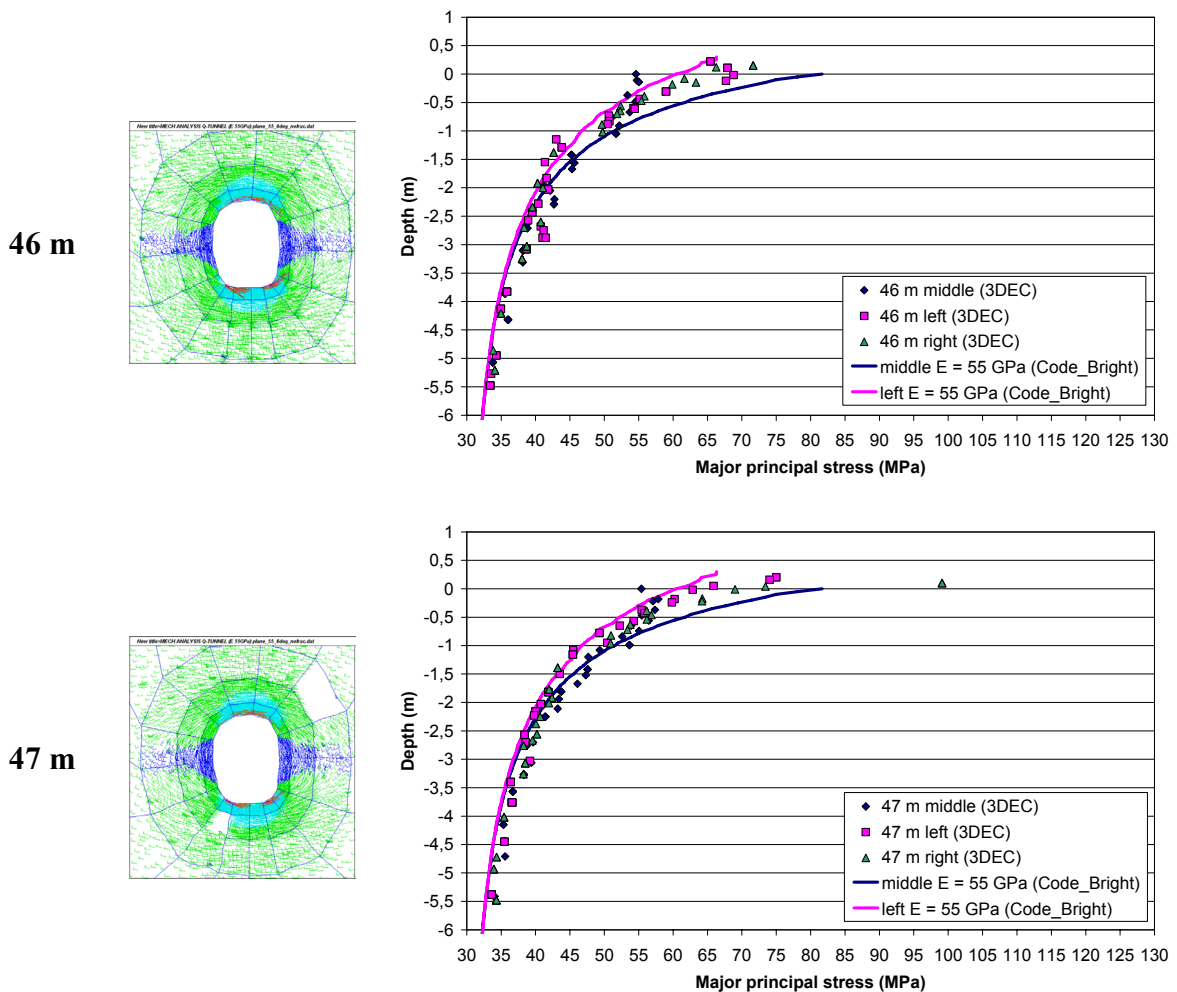
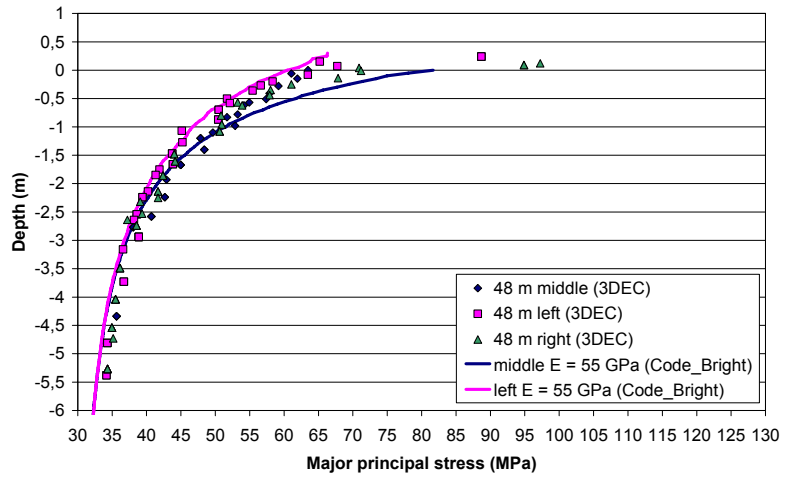
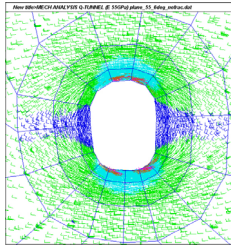
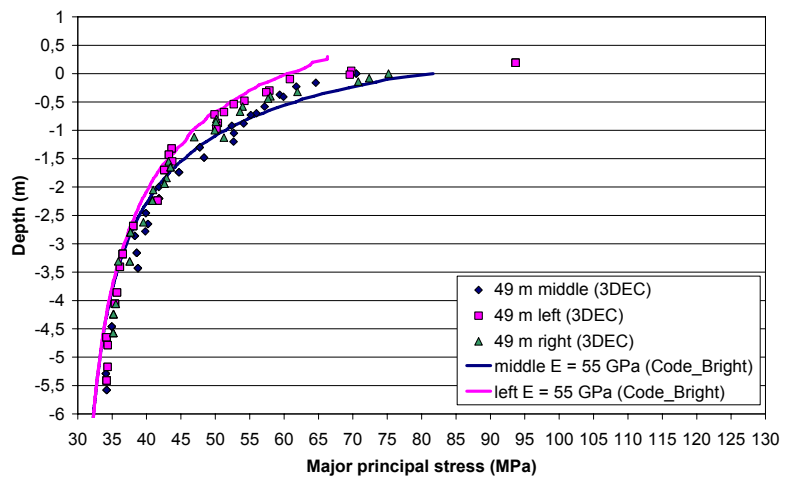
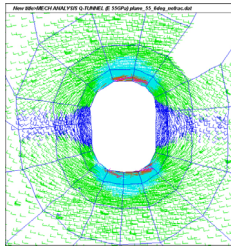


**Figure A-4.** Major principal stress along vertical scan lines in tunnel segments 46 to 55 in the Q-tunnel. 3DEC results from /Mas Ivars, 2008/.

48 m



49 m



50 m

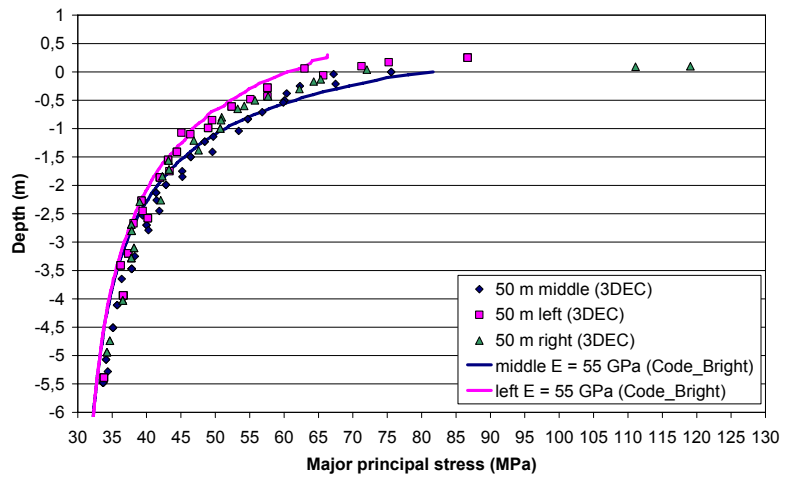
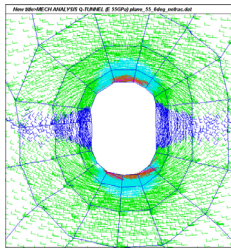
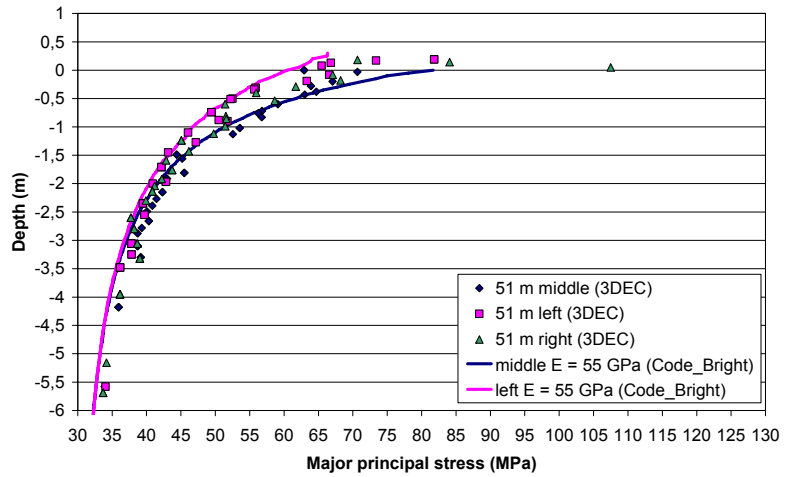
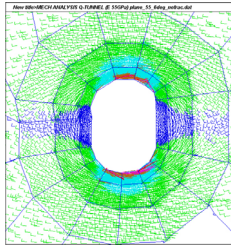
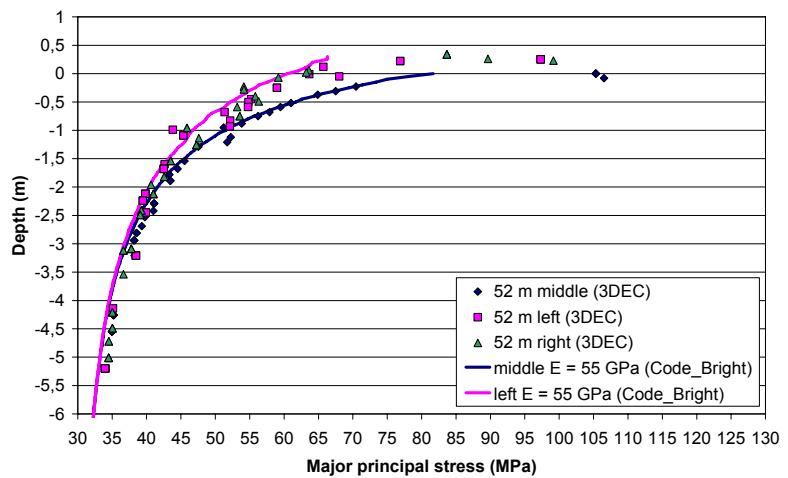
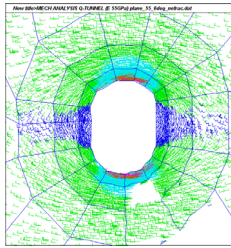


*Figure A-4 continued. Major principal stress along vertical scan lines in tunnel segments 46 to 55 in the Q-tunnel. 3DEC results from /Mas Ivars, 2008/.*

51 m



52 m



53 m

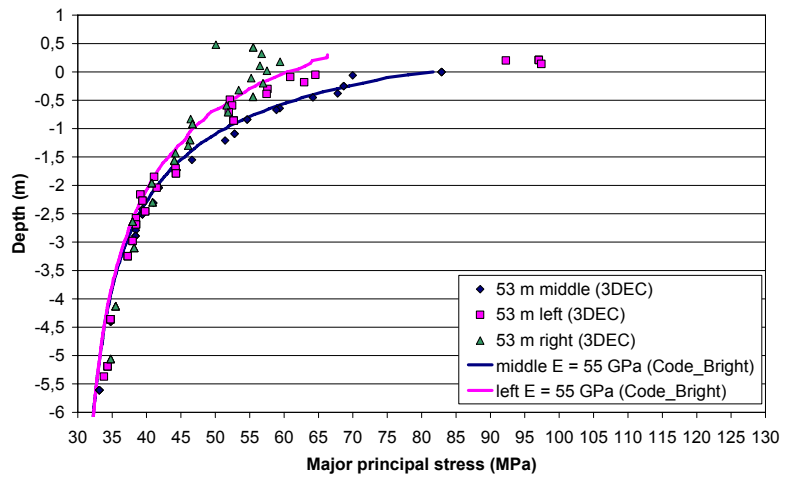
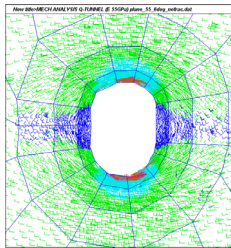
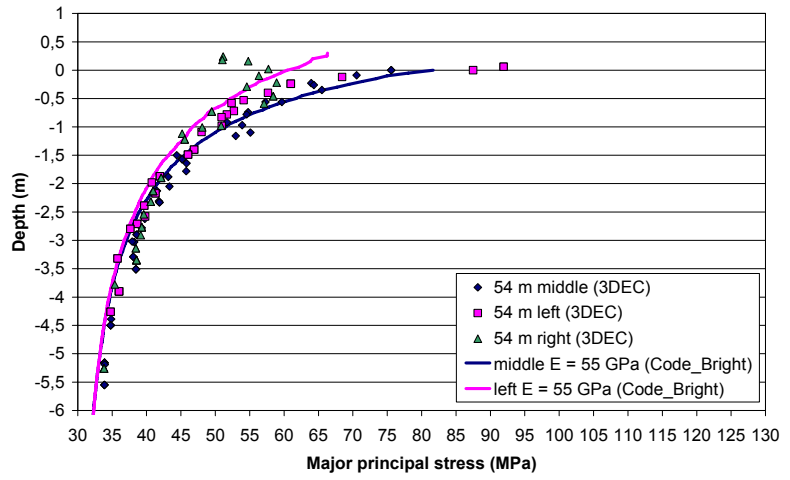
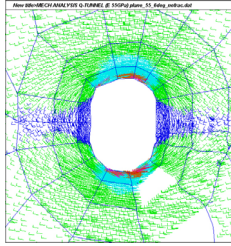
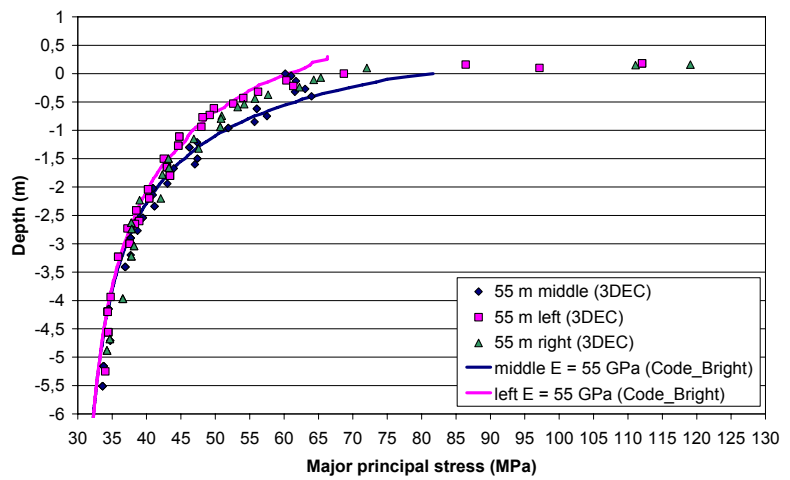
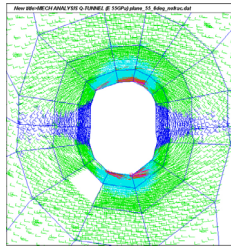


Figure A-4 continued. Major principal stress along vertical scan lines in tunnel segments 46 to 55 in the Q-tunnel. 3DEC results from /Mas Ivars, 2008/.

54 m



55 m



*Figure A-4 continued. Major principal stress along vertical scan lines in tunnel segments 46 to 55 in the Q-tunnel. 3DEC results from /Mas Ivars, 2008/.*